

# A push-pull double-contact MEMS relay fabricated by MetalMUMPs process

Lifeng Wang<sup>1</sup> · Yue Jin<sup>1</sup>

Received: 25 February 2016 / Accepted: 24 May 2016 / Published online: 30 May 2016  
© Springer-Verlag Berlin Heidelberg 2016

**Abstract** This document presents a push-pull double-contact MEMS (Micro ElectroMechanical System) relay. The MEMS relay is electrostatic driven and laterally actuating. Two push-pull structures form two parallel contacts for the proposed MEMS relay, which can make the contact resistance of the MEMS relay be smaller. The push and pull actions of the push-pull actuators can be accomplished simultaneously using only one action signal. In addition, high inductance DC bias line and substrate removal are used for additional electrical and/or thermal isolation. The fabrication of the proposed switch is based on the standard MetalMUMPs process. The measured pull-in voltage is 116 V and the switch-ON delay is 44  $\mu$ s. Contact resistance of the MEMS relay is less than 1  $\Omega$  when the stress voltage exceeds 120 V.

## 1 Introduction

Due to the progress and development in micro-machining field, MEMS (microelectromechanical system) relays have been demonstrated in the 1970 s for the first time (Peterson 1976). Because of the potential applications in automatic test equipment systems, medical instruments and ground/space wireless communication systems, various MEMS relays and RF/microwave MEMS switches are reported from then on (Zavracky et al. 1999; Wang et al. 2013; Ma et al. 2015). To enhance the performances, the push-pull structure is applied in MEMS relays. By using the push and

pull movements of leverages and torsion springs, high isolations (Hah et al. 2000) or high  $C_{\text{off}}/C_{\text{on}}$  ratio (Rangra et al. 2005) or high power handing (Song et al. 2012) MEMS relays are demonstrated. By using magnetostatic latching and electrothermal actuation, a bistable push-pull MEMS switch with lower power consumption is reported (Wu et al. 2010). However, the toggle and the leverage structures of these push-pull MEMS relays are not only hard to process but also complex to control.

To retain the advantages of the push-pull method while avoiding its disadvantages, a push-pull double-contact MEMS relay is designed and fabricated by the MetalMUMPs process. The thick nickel MetalMUMPs process, chosen here, is very suitable for complicated in-plane moving structures (Cao et al. 2007; Almeida et al. 2007). In Sect. 2, the configuration and the principle of the MEMS relay is proposed. Contents in Sect. 3 describe the measurement and the verification of the MEMS relay. Finally, conclusion is given in Sect. 4.

## 2 Configuration and principle

The schematic view of the push-pull double-contact MEMS relay is shown in Fig. 1. The MEMS relay consists of four moveable beams, four electrostatic-driven actuators, two contact parts, one DC bias line and input/output AC ports. Both AC ports are anchored to substrate and are connected to the movable beams. The end of each moveable beam is connected and driven by a differential parallel plate actuator. The four actuators share one electrode which is connected to the DC bias pad. The other electrodes of the four actuators are connected to the left AC ports and the right AC ports, respectively.

✉ Lifeng Wang  
wanglifeng@seu.edu.cn

<sup>1</sup> Key Laboratory of MEMS of the Ministry of Education, Southeast University, Nanjing 210096, China

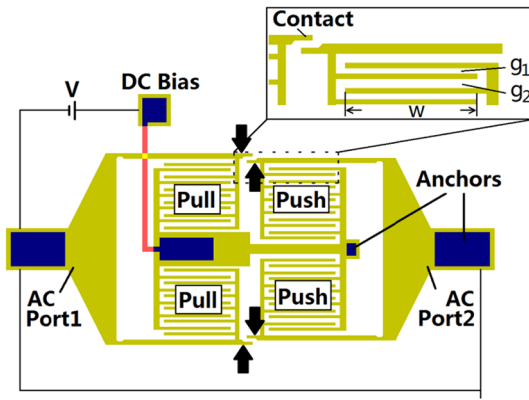


Fig. 1 A schematic view of the proposed MEMS relay

There are four actuators in the proposed MEMS relay, the two actuators on the left side are designed to pull and the other two on the right side are designed to push. Hence, two push-pull structures are included in the proposed MEMS relay. By using two parallel push-pull structures here, two benefits are brought. First one, the gap distance of each contact structure is increased. Second one, two contacts in parallel connection could lead to smaller contact resistance of the MEMS relay. Smaller contact resistance is obviously better for a relay, and larger contact gap means better isolation between input and output AC signals. Another attractive feature of this design is that, its push and pull actions can be accomplished simultaneously at only one step. This is because that, all the high potentials of the four actuators are connected to one common DC bias line, and their low potentials are all connected to input/output AC ports that are set to DC ground potential here.

The four electro statically-driven actuators and movable beams are designed exactly the same. Hence, only one of them needs to be investigated. The calculation formula of pull-in voltage of the differential parallel plate actuator can be given as (Rebeiz 2003),

$$V_p = \sqrt{\frac{8k}{27\epsilon_0 w t n} g_0^3} \tag{1}$$

where  $w$  is the overlapping length of the comb fingers,  $t$  is their thickness,  $n$  is the number of their pairs,  $k$  is the spring constant of the cantilever beam and  $g_0$  represents the equivalent air gap. The equivalent air gap  $g_0$  can be approximated as (Wang et al. 2012),

$$\frac{1}{g_0^2} \approx \frac{1}{g_1^2} - \frac{1}{g_2^2} \tag{2}$$

where  $g_1$  and  $g_2$  are the small and large gaps of the actuators, respectively, as shown in Fig. 1.

Table 1 Parameters of a differential parallel plate actuator

Parameter	$g_1$ ( $\mu\text{m}$ )	$g_2$ ( $\mu\text{m}$ )	$w$ ( $\mu\text{m}$ )	$n$
Value	9	15	207	6

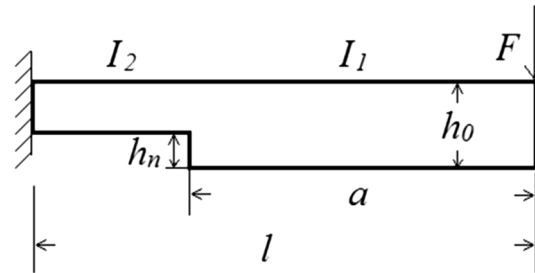


Fig. 2 The simplified model of the movable beam for analytical calculation

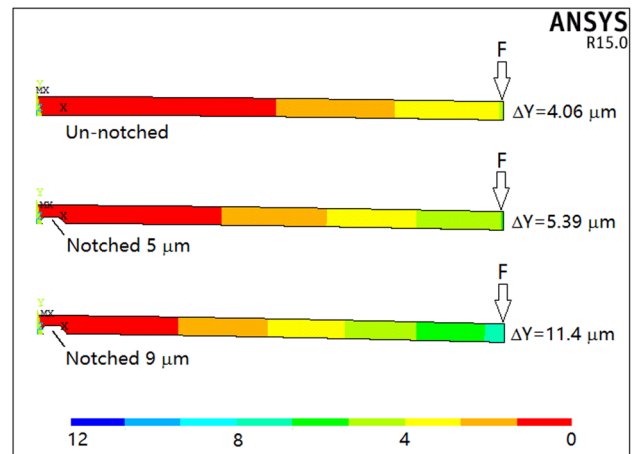


Fig. 3 FEM simulation of the moveable beams with different notch depth

Table 1 gives the design parameters of the differential parallel plate actuators of the MEMS relay.

To reduce the pull-in voltage, the moveable beams are notched near their anchors. The spring constant of moveable beams with different notch depth will be calculated by analytical calculation, and also be simulated by ANSYS simulation for comparison.

In order to facilitate the derivation of analytical formula, the notched movable beam is simplified as shown in Fig. 2. In which,  $l$  is the length of the movable beam,  $a$  is the length of the un-notched part of the beam,  $h_0$  is the width of the un-notched part,  $h_n$  is the depth of the notch,  $I_1$  is the moment of inertia of the un-notched part and  $I_2$  is the moment of inertia of the notched part.

Because the beam is moving laterally, the moment of inertia of the beam  $I$  can be calculated as,

$$I = th^3 / 12 \tag{3}$$

where  $t$  is the thickness of the movable beam, as we defined above, and  $h$  is the width of the beam.

According to the theory of elasticity (Young and Budynas 2002), the formula for spring constant  $k$  can be obtained as,

$$k = \frac{3EI_2}{l^3 - \left(1 - \frac{l_2}{l_1}\right)a^3} \tag{4}$$

Set  $l = 380 \mu\text{m}$ ,  $t = 20 \mu\text{m}$ ,  $a = 362 \mu\text{m}$ ,  $h_0 = 15 \mu\text{m}$  and  $h_n = 0, 5$  and  $9 \mu\text{m}$ , respectively. The Young's module and the Poisson ratio are set to 160 GPa and 0.24 (He et al. 2009). Using Eq. (3) together with (4), the spring constant  $k$  could be calculated as 49.1, 37.2 and 16.5 N/m, respectively.

ANSYS simulation of moveable beams with different notch depth is shown in Fig. 3. Here, the shape of the notch is not simplified. A 200  $\mu\text{N}$  force is stressed at the right end of each moveable beam. According to the simulation results in Fig. 3, the spring constants of the un-notched, 5  $\mu\text{m}$  notched and 9  $\mu\text{m}$  notched moveable beams are 49.1, 37.1 and 17.5 N/m, respectively. It could be seen that the analytical calculated results and the FEM simulation results are basically consistent. The error between them is mainly caused by the model simplification of the notch during analytical calculation.

Both the analytical calculation and the FEM simulation show that, the spring constant of the moveable beam greatly decreases as the notch depth increases. Hence, the moveable beam will be notched to the minimum size that fabrication process allows.

The other way to reduce the actuation voltage is provided by the MetalMUMPs process. In MetalMUMPs process, the sidewall of the nickel structures could be coated by electroplated gold to reduce their contact resistances. Here, the sidewall coating electroplated gold could be used to reduce the gap distances of the actuators, and thus lead to smaller actuation voltage. However, the thickness of the electroplated gold could not be designed as a certain value, it ranges between 1 and 3  $\mu\text{m}$ . Due to the sidewall coating process, the final gap distances of the actuator will be smaller than the designed parameters in Table 1.

Furthermore, because of the coating of the electroplated gold layer, the fabricated moveable beam is actually a double layer structure. However, the electroplated gold layer is thin and pretty soft. So the double layer structure is simplified to a single layer nickel structure for the convenient of calculation and simulation. Due to this simplification, the calculated and simulated results are just approximate for the fabricated MEMS relay.

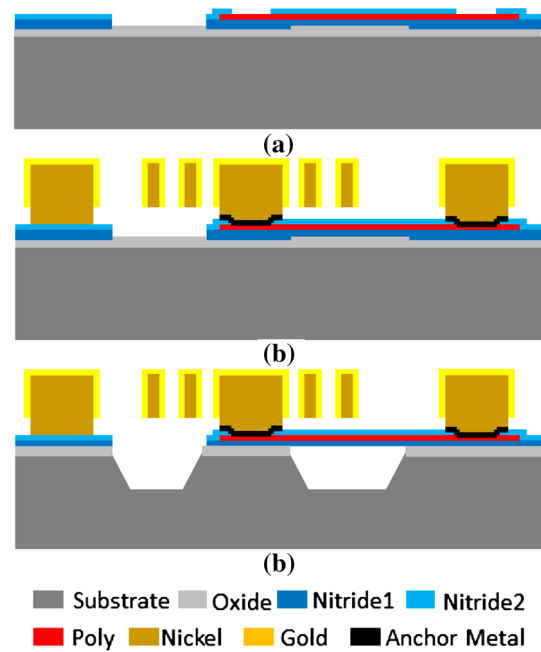


**Fig. 4** Fabrication Process of the MEMS relay using MetalMUMPs process. **a** This step forms the cross-over DC bias line of the MEMS relay. **b** This step forms the main structures of the MEMS lay, including the actuators, the contacts and IO ports. **c** This step releases the MEMS relay

### 3 Validation and measurements

The proposed push-pull double-contact MEMS relay is fabricated by MetalMUMPs process. The MetalMUMPs process is an electroplated nickel surface micromachining process (MUMPs® 2014). Figure 4 shows the main process steps of the MEMS relay using MetalMUMPs process. Figure 4a, a 2  $\mu\text{m}$  thick oxide is grown on the surface, followed by deposition and wet etching of a 0.5  $\mu\text{m}$  thick sacrificial phosphosilicate glass (PSG) layer. Then, A 0.35  $\mu\text{m}$  layer of silicon nitride is deposited, followed immediately by the deposition and patterning of a 0.7  $\mu\text{m}$  layer of poly-silicon. After that, a second 0.35  $\mu\text{m}$  layer of silicon nitride is deposited and patterned. This step forms the cross-over DC bias line of the MEMS relay. Figure 4b, a thin metal layer consisting of 10 nm Cr and 25 nm Pt is deposited and patterned. Then, Nickel is electroplated to a nominal thickness of 20  $\mu\text{m}$  using a patterned resist stencil. Similar as the Nickel electroplating process, a 1–3  $\mu\text{m}$  gold layer is electroplated. This step forms the main structures of the MEMS lay, including the actuators, the contacts and IO ports. Figure 4c, to release the moveable structures, a 49% HF solution is used to remove the PSG sacrificial layers and the Isolation Oxide layer. Finally, the silicon substrate is wet etched to form a 25  $\mu\text{m}$  deep trench.

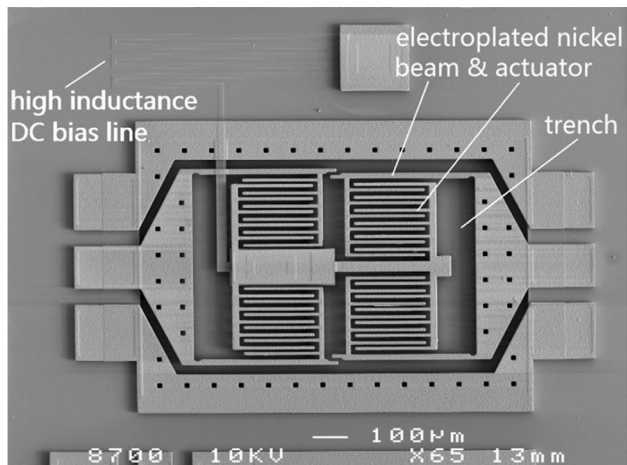


**Fig. 5** A SEM picture of the fabricated push-pull double-contact MEMS relay

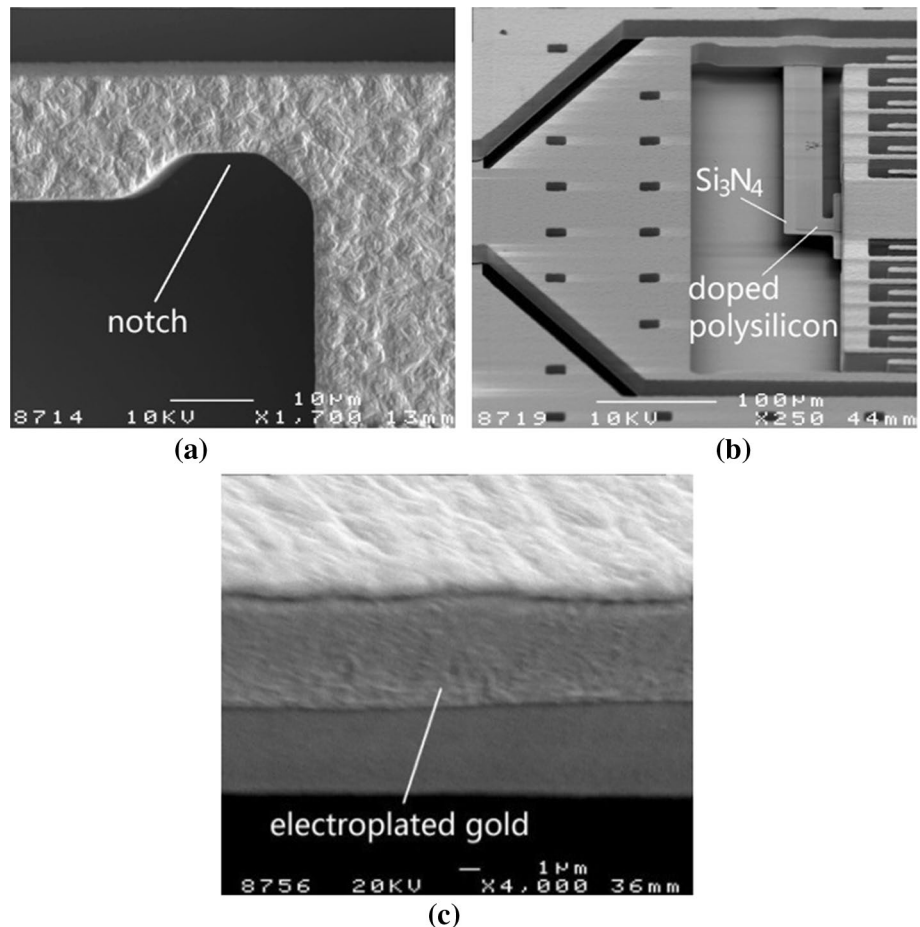
The SEM picture of the fabricated push-pull MEMS relay is shown in Fig. 5. The primary structural and electrical layer is the 20  $\mu\text{m}$  electroplated nickel layer, and a 1–3  $\mu\text{m}$  electroplated gold layer is used to coat the

sidewalls of nickel structures for smaller gap distance and lower contact resistance. The cross-over electrical routing layer is the doped polysilicon layer. The trench layer in the silicon substrate is incorporated for additional thermal and electrical isolation. For better separating the DC signals from the AC signals, the DC bias line is designed to be the high-inductance mender shape. The two metal lines besides the MEMS relay could be used as AC ground for high frequency AC signals. The size of the push-pull double-contact MEMS relay shown in Fig. 5 is about  $1.4 \times 1.1 \text{ mm}^2$ .

Details of the fabricated MEMS relay are shown in Fig. 6. Figure 6a shows that, the movable beam is notched to 9.2  $\mu\text{m}$  width near its anchor. Figure 6b shows the cross-over DC bias line beneath the thick nickel structures. The 0.7  $\mu\text{m}$  doped polysilicon DC bias line is wrapped by two 0.35  $\mu\text{m}$   $\text{Si}_3\text{N}_4$  layers for electrical isolation. Figure 6c shows the sidewall of the thick Nickel is coated by electroplated gold. The actual thickness of the fabricated sidewall coating electroplated gold layer is about 1.3  $\mu\text{m}$ .

The actuation voltage and the switching delay of the MEMS relay are tested. The saw-tooth waves are used for actuation voltage test, and the square waves are used

**Fig. 6** Details of the fabricated MEMS relay, **a** moveable beam is notched near the anchor, **b** the cross-over DC bias line beneath the thick nickel structures, **c** the sidewall coating electroplated gold



for switching delay test. Both test waveforms are generated by the Agilent 33220A Function/Arbitrary Waveform Generator together with the NF BA4825 High Speed Bipolar Power Amplifier. The drive signal and the test signal are both observed through a digital storage oscilloscope. The measurement results of the actuation voltage and the switching delay of the MEMS relay are shown in Fig. 7. Figure 7a shows the pull-in and pull-off voltage of the MEMS relay is 116 V and 80 V, respectively. Figure 7b shows the measured switching delays of the MEMS relay are 44 and 36 μs for the transition from OFF to ON state and for the transition from ON to OFF state, respectively.

As we mentioned above, the small gap  $g_1$  and the large gap  $g_2$  will decrease after fabrication. The measured  $g_1$  and  $g_2$  of the fabricated actuators are 6.2 and 12.2 μm, respectively. Using Eq. (2), the equivalent air gap  $g_0$  can be calculated as 7.4 μm. Substituting these measured parameters and the parameters in Table 1 into Eq. (1), the spring constant of the fabricated movable beam could be calculated as 24.6 N/m.

The measured contact gap is 8.8 μm, so the travel distance of each actuator is 4.4 μm. By using the simulated spring constant, the recovery force can be easily calculated as 108.2 μN.

When the MEMS relay is closed, the small gap of the actuator can be reduced to 1.8 μm, and the large gap is increased to 16.6 μm. At this situation, the electrostatic force generated by the large gaps are very small compared with the one generated by the small gaps (about 1/85), so the former could be ignored here. By using the measured parameters and the parameters in Table 1, the electrostatic force can be calculated as 456.5 μN. So the contact force is 348.3 μN.

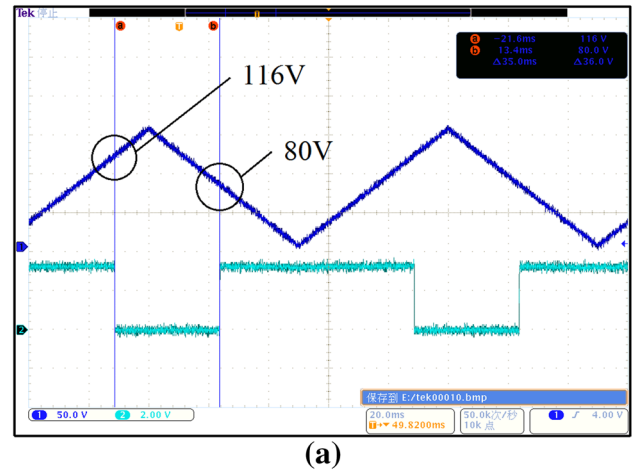
The quality factor of vertically actuating structures (e.g., surface sacrificial fabricated cantilevers) can be measured by Laser Doppler Vibration (LDV) system. But the LDV system is not suitable for our laterally moving structures. However, we can approximately calculate the quality factor from the structure parameters, and the measured results.

Firstly, the damping coefficient  $b$  can be calculated by (Rebeiz 2003),

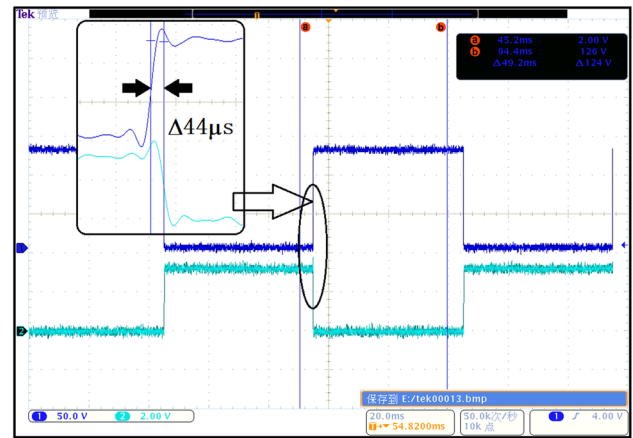
$$b = \frac{3\mu_a(wtn)^2}{2\pi g_1^3} \tag{5}$$

where  $\mu_a$  is the viscosity of ideal gases at STP (standard temperature and pressure),  $\mu_a = 1.845 \times 10^{-5}$  Pa s. Substitute structure parameters of the actuator into Eq. (5), the damping coefficient  $b$  can be calculated as  $2.3 \times 10^{-5}$ . When the damping coefficient is very small (close to zero), the switching ON delay can be approximately calculated as (Rebeiz 2003),

$$t_s = \frac{3.67}{2\pi f_0 V_s / V_p} \tag{6}$$



(a)



(b)

Fig. 7 The measurement result of the MEMS relay. a The actuation voltage of the MEMS relay, b the switching time of the MEMS relay

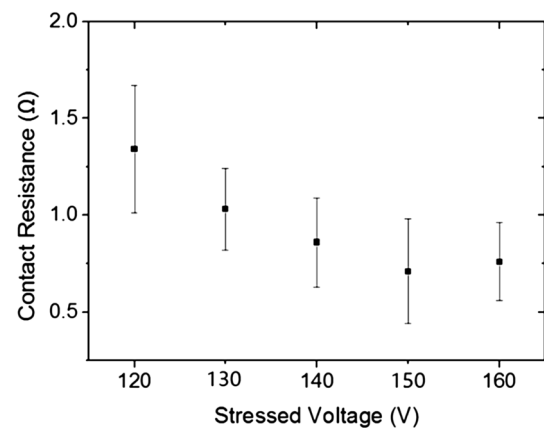


Fig. 8 The variation of the contact resistance of the MEMS relay under different stress voltages



where  $V_s$  is the applied voltage and  $V_p$  is the pull-in voltage. Here, we set  $V_s/V_p=1$ . Substitute the measured switching ON time into Eq. (6), the resonant frequency of the MEMS relay is obtained as 13.3 kHz.

The expression of the quality factor  $Q$  is given by,

$$Q = \frac{k}{2\pi f_0 b} \quad (7)$$

Finally, the quality factor of the MEMS relay can be calculated as 12.8.

The ON-resistance of the MEMS relay is also measured using Fluke 8808A Digital Multimeter. Figure 8 shows the measured contact resistance of the MEMS relay under different stress voltages. Contact resistance less than 1  $\Omega$  is achieved except the 120 V stress voltage. It can be seen that the contact resistance decreases as the stress voltage increases. The smaller resistance at higher actuation voltage could be explained by the rough surface of the sidewall coating gold layer (Almeida et al. 2007). Higher stress voltage can lead to higher contact force, and thus larger contact area between two rough electroplated gold surfaces.

## 4 Conclusion

An electrostatic driven push-pull double-contact MEMS relay is designed, fabricated and tested. Two push-pull structures are included in the proposed MEMS relay, and the push and pull actions can be accomplished simultaneously using only one action signal. In addition, high-inductance DC bias line and substrate removal are used for additional electrical and/or thermal isolation. The fabrication process of the proposed switch is the standard MetalMUMPs process. The measured pull-in voltage is 116 V and the switch-ON delay is 44  $\mu$ s. Contact resistance of the MEMS relay is less than 1  $\Omega$  when the stress voltage exceeds 120 V. Hence, the MEMS relay we demonstrate here has the advantages of simpler controlling and easier processing, comparing with reported push-pull MEMS relays. However, the actuation voltage is not very satisfactory, and the improvement method, such as increase the number of the comb pairs, worth a try.

**Acknowledgments** This work is supported by the National Natural Science Foundation of China (61401084) and the National High Technology Research and Development Program of China (2015AA042602).

## References

- Almeida L, Ramadoss R, Jackson R, Ishikawa K, Yu Q (2007) Laterally actuated multicontact MEMS relay fabricated using MetalMUMPs process experimental characterization and multiscale contact modelling. *J Micro/Nanolith MEMS MOEMS* 6(2):02300901–02300910
- Cao A, Yuen P, Lin L (2007) Microrelays With Bidirectional Electrothermal Electromagnetic Actuators and Liquid Metal Wetted Contacts. *J Microelectromech S* 16(3):700–708
- Hah D, Yoon E, Hong S (2000) A low-voltage actuated micromachined microwave switch using torsion springs and leverage. *IEEE T Microw Theory* 48(12):2540–2545
- He SY, Chang JS, Li LH, Ho H (2009) Characterization of Young's modulus and residual stress gradient of MetalMUMPs electroplated nickel film. *Sensor Actuat A-Phys* 154:149–156
- Ma B, You Z, Ruan Y, Chang S, Zhang G (2015) Electrostatically actuated MEMS relay arrays for high-power applications. *Microsyst Technol*. doi:10.1007/s00542-015-2660-y
- MUMPs® process (2014) MetalMUMPs Design Handbook Rev. 4.0. <http://www.memscap.com/products/mumps/metalumps/reference-material>, accessed June 2014
- Peterson KE (1976) Micromechanical membrane switches on silicon. *IEEE T Electron Dev* 23(4):376–386
- Rangra K, Margesin B, Lorenzelli L, Giacomozzi F, Collini C, Zen M, Soncini G, Tin L, Gaddi R (2005) Symmetric toggle switch—a new type of rf MEMS switch for telecommunication applications: design and fabrication. *Sensor Actuat A Phys* 123–124:505–514
- Rebeiz GM (2003) *RF MEMS Theory Design and Technology*. Wiley, Hoboken
- Song YH, Han CH, Kim MW, Lee JO, Yoon JB (2012) An Electrostatically Actuated Stacked-Electrode MEMS Relay With a Levering and Torsional Spring for Power Applications. *J Microelectromech S* 21(5):1209–1217
- Wang LF, Han L, Tang JY, Huang Q A (2012) Fabrication of a Push-Pull Type Electrostatic Comb-Drive RF MEMS Switch. *IEEE 11th Int Conf on Sensors, Taipei*, pp. 331–334
- Wang LF, Han L, Tang JY, Huang QA (2013) Lateral contact Three-State RF MEMS switch for ground wireless communication by actuating rhombic structures. *J Microelectromech S* 22(1):10–12
- Wu YB, Ding GF, Zhang CC, Wang J, Mao SP, Wang H (2010) Magnetostatic bistable MEMS switch with electrothermal actuators. *Electron Lett* 46(15):1074–1075
- Young WC, Budynas RG (2002) *Roark's Formulas for Stress and Strain*, 7th edn. McGraw-Hill, New York
- Zavracky PM, McGruer NE, Morrison RH, Potter D (1999) Microswitches and microrelays with a view toward microwave applications. *Int J RF Microw C E* 9(4):338–347